Microelectronics Reliability 53 (2013) 906–911

Contents lists available at SciVerse ScienceDirect

Microelectronics Reliability

journal homepage: www.elsevier.com/locate/microrel

Characteristics of size dependent conductivity of the CNT-interconnects formed by low temperature process

Wei-Chih Chiu *, Bing-Yue Tsui

Department of Electronics Engineering and Institute of Electronics, National Chiao Tung University, No. 1001, Ta-Hsueh Road, Hsinchu 30010, Taiwan, ROC

ARTICLE INFO

Article history:
Received 16 November 2012
Received in revised form 5 March 2013
Accepted 5 March 2013
Available online 12 April 2013

ABSTRACT

In this paper, a simple and low temperature fabrication process, slow spin rate coating and dry etching, is proposed to construct the CNT-interconnects for future VLSI interconnect applications. Two sets of CNT-interconnects named width and length varying interconnects were fabricated to investigate the characterization of size dependent conductivity of CNT-interconnects. Not only the amount of the CNT solution spin-coated for forming the CNT networks but also the area of CNT-interconnect regime would affect the conductance, variation, and conductive probability of CNT-interconnects. The yield of working CNT-interconnects does not show direct relation with the conductive probability or the amount of the CNT solution for CNT network formation. Based on the percolation theory, we characterize the average conductance of size-varying CNT-interconnects by three regions: percolation region, power region and linear region. In addition, as the density within a specified CNT-interconnect regime accumulates, the conductive behavior would be eventually characterized as a conventional resistor.

1. Introduction

Copper has been the dominant interconnect material in the VLSI technology since the late 1990s due to the excellent bulk conductivity of 5.88×10^5 S/cm and electromigration reliability [1]. Over many technological generations, the device dimensions now proceed into nanometer regime. However, continued scaling down of the integrated circuit has been degrading the performance of Cu-interconnects. According to the experiments proposed by Liu et al. [2], the conductivity of copper film would decrease to 3.09×10^4 S/cm as the thickness reduces to 11.5 nm. Constantly shrinking the thickness to less than 10 nm, the copper film would be in the form of many discontinuous islands which, in turn, causes resistivity to surge to an extremely high extent. Besides, in 2004, Rossnagel further proposed that the thickness dependent "size effect" including electron-surface scattering, grain boundary scattering and surface roughness-induced scattering would alter the conductivity of copper by simulation [3]. Furthermore, the occurrence of electromigration would also seriously influence the reliability of Cu-interconnects as the size of the deposited copper grains reduces [4]. Apart from the defects from the size effects, the fabrication method for Cu-interconnects was also an enormous obstacle for engineers since the copper cannot be patterned by dry etching. Although the damascene process has become the industry standard for Cu-interconnects' fabrication [5], the diffusion of the Cu atom into the surrounding dielectric and silicon substrate would deteriorate the device performance as the dimensions of interconnect are continuously being scaled [6]. Therefore, looking for new materials which can replace Cu as interconnects is a critical issue.

In recent years, carbon nanotubes (CNTs) have emerged as an ideal material for post-Si technology mainly due to the exceptional electrical properties [7–10]. For instance, a single metallic carbon nanotube with diameter of 1 nm can theoretically pass about 2.4×10^8 A/cm^2 of current density without adverse effects which is approximately one thousand times more than copper [11]. Such an excellent current capability shows great potential for electronic application [12–16]. However, the variations of carbon nanotubes arising from non-idealities in the CNT synthesis process have been the major drawback to mass reproduction [17]. By ensemble averaging over the large quantity of individual tubes, the tube-to-tube resistance variation could be effectively reduced according to much past research [18]. Additionally, the electronic application of random interconnected network of CNTs not only retains remarkable properties but also provides a relatively simple fabrication process. Previous studies were able to construct CNT networks by spin coating [19], vacuum filtration [20], printing method for transferring to a flexible plastic substrate [21], and directly growing on dispersed catalyst with CVD at temperatures greater than 400 °C [22]. However, the enhancement of CNT network conductivity has still posed great challenges on the further advancement of carbon nanotube electronics. The low conductivities could mainly be due to tube defects [23], low graphitization [24], the presence of high junction resistances between metallic and semiconducting CNT [25] and poorly dispersed film. In 2011, Zhenen Bao's group

* Corresponding author. Tel.: +886 734 747 0177; fax: +886 3 5131570.
E-mail address: chiweich@umich.edu (W.-C. Chiu).

0026-2714/$ - see front matter © 2013 Elsevier Ltd. All rights reserved.
http://dx.doi.org/10.1016/j.microrel.2013.03.001

developed an effective method to enhance the conductivity of spin-coated CNT networks by depositing CNT on three types of substrates (silicon, glass, and polyethylene terephthalate (PET)) that were treated with amine-rich poly-L-lysine (PLL). The results show that they have improved the sheet conductance of spin-coated CNT networks to about 7×10^{-5} S [26]. This work attempts to address a simple and low temperature fabrication process, slow spin rate coating and dry etching, to construct various sizes of CNT-interconnects and demonstrate the size associated characteristics of the conductance, variations, and conductive probability of the CNT-interconnects. In addition, the transition of CNT-interconnect electrical properties resulting from different times of coating cycles and the area of CNT-interconnect regime will be shown and interpreted by percolation theory as well.

2. Experiments

Two sets of CNT-interconnects were designed for the size dependent conductivity investigation as illustrated in Fig. 1a. The CNT-interconnects in the first set have fixed length at 100 μm with width varying from 5 μm to 500 μm, while the other set has fixed width at 5 μm with length varying from 5 μm to 1000 μm. The former set is named width varying CNT-interconnects and the number of squares is in the range of 0.2–20. The latter is named length varying CNT-interconnects and the number of squares is in the range of 1–200. The square number, the length of interconnect (L) divided by the width of interconnect (W), is a common factor for designing interconnects in the VLSI technology. The conductance of each CNT-interconnect was measured by a four-terminal bridge resistor as depicted in Fig. 1b. The starting material, boron-doped (100)-oriented 4-inch-diameter silicon wafer, was first capped by a 200-nm-thick thermal oxide and followed by a 1-nm-thick layer of Al_2O_3 deposited by an atomic-layer deposition (ALD) system in order to improve the uniformity of CNT distribution [27,28]. In this experiment, we adopted AP-grade CNT powder commercially available from Carbolex which contains the CNTs with an average diameter of 1.4 nm and an average length of 3.5 μm. The distribution of the semiconducting and metallic CNT in the powder is about 2:1 as determined by Raman spectroscopy [29]. In addition, the purity of CNT powder is 50–70% with residue catalyst Yttrium (Y) and Nickel (Ni). The CNT solution for the experiment was prepared by dissolving 2 mg arc discharge grown CNTs in dimethylformamide (DMF) solvent and then was uniformly dispersed by 24 h sonication. By several coating cycles, uniform and dense CNT networks were expected. In each cycle, about 0.5 mL of the CNT solution was first dropped at the wafer center, and then the wafer was spun by the spin speed of 100 rpm for 10 s and followed by a 120 °C baking to evaporate the DMF solvent entirely. The CNT networks formed on the wafer after 40 cycles (20 mL) are shown in SEM image of Fig. 1c. From several images, the average spin-coated CNT density per unit area by the amount of 20 mL CNT solution could be approximated about 8.5 CNTs/μm^2 by manually counting. The four-terminal bridge resistors for conductance measurement were fabricated by depositing 60 nm Pd/Ti metal with the ratio about 9/1 by a sputtering technique and patterned by a lift off process. Finally, the CNT-interconnect regimes were specified by O_2 plasma etching. The main process flow of CNT-interconnect construction is illustrated in Fig. 2.

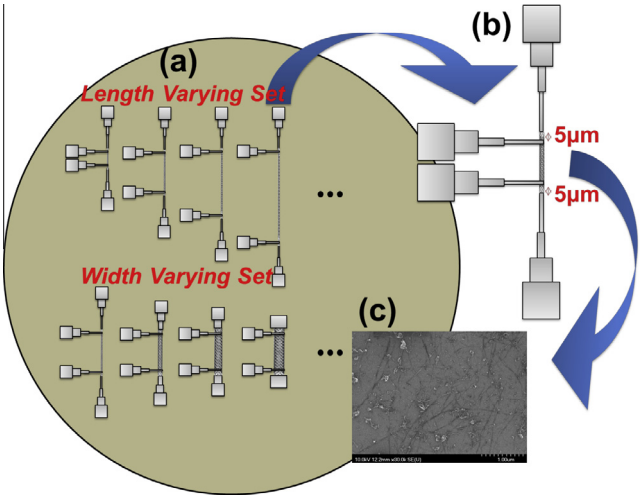

Fig. 1. Schematic array of four-probe bridge resistors: (a) Illustration of the CNT-interconnects in length varying set has length varying from 5 μm to 1000 μm with 5 μm fixed in width and the CNT-interconnects in width varying set has width varying from 5 μm to 500 μm with 100 μm fixed in length. (b) Schematic diagram of four-probe resistors designed for this work. Adjacent two probes are designed to have about 5 μm of space for precise measurement. (c) SEM image of the CNT network fabricated by 40 cycles of spin coating in interconnect regime.

3. Results and discussion

3.1. Conductance distribution of the CNT-interconnects

Fig. 3a and b shows the conductance distribution of the width and length varying CNT-interconnects, respectively, fabricated by the amount of 10 mL (20 coating cycles), 20 mL (40 coating cycles), and 80 mL (160 coating cycles) CNT solution. The statistical distribution shows that the conductance of every CNT-interconnect is apparently enhanced by the increase of the times of coating cycles. It can be understood that the more CNTs randomly distributed in the CNT networks, the higher the probability for CNTs to connect conductive paths. Moreover, the sheet conductance of the CNT-interconnects formed by the amount of 10 mL, 20 mL, and 80 mL CNT solution ranges from 3.42×10^{-6} to 8.05×10^{-5} S, 1.50×10^{-5} to 1.21×10^{-4} S, and 7.40×10^{-5} to 2.09×10^{-4} S, respectively. It is known that the interconnects between two metallic or two semiconducting CNTs have lower resistances than a metallic/semiconducting interface [30]. This would affect the conductivity of the CNT-interconnects because the carrier transportation in a CNT random network is dominated by the Schottky emission [27]. It is noted that except for some points with extreme values, the conductance variations of each size of CNT-interconnect mostly become narrow as the times of coating cycle increase. Additionally, most of the CNT-interconnects fabricated by the amount of 80 mL CNT solution have the conductance variation around one order. These results verify that the CNT network is effective to lower the variation as the CNT density increases in the interconnect regime. These results further show that the CNT-interconnects with the size of $L \times W = 1000\ \mu m \times 5\ \mu m$ are probable to be conductive and possess the average conductance approximately 5.22×10^{-7} S as shown in Fig. 3b.

Compare Fig. 3a with b, under the same square number of CNT-interconnects and the same coating cycles for CNT networks formation, the CNT-interconnects with a smaller area of interconnect regime mostly possess lower conductance and larger variation. The results could be interpreted that the spin coating technique and the 1-nm-thick layer of Al_2O_3 could facilitate the uniformity of CNT dispersion on the wafer, but the distribution of CNT conductive paths within the specific CNT-interconnects with the same square number might not be the same once the interconnect regimes were specified. In terms of the probability, the CNT-interconnects with larger interconnect area is likely to contain more end to end CNT conductive paths.

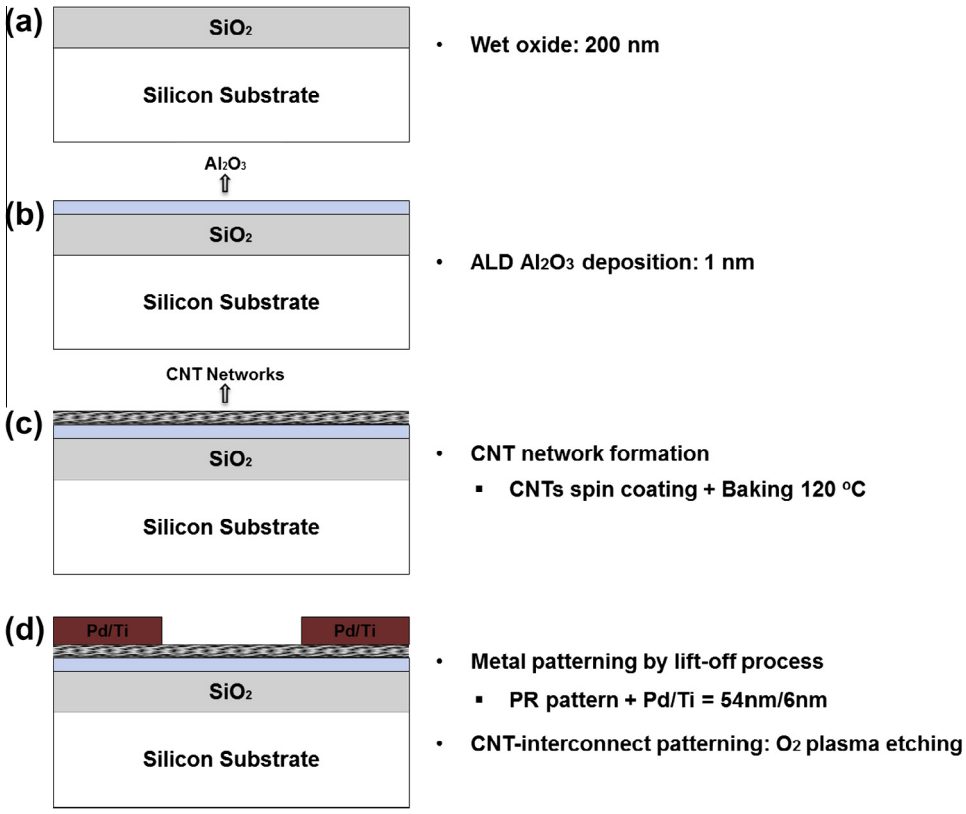

Fig. 2. Main process flow for conductance of the CNT-interconnects measurement: (a) after wet oxide growth, (b) after 1-nm-thick layer of Al_2O_3 growth by ALD for uniform distribution of the CNT networks, (c) after formation of the CNT film and baking process, (d) after sputtering and lift-off techniques for bridge resistors patterning and O_2 plasma etching for interconnect specification.

3.2. Conductive probability statistics of the CNT-interconnects

Fig. 4a and b shows the histograms of the yield of working width and length varying CNT-interconnects versus the square number of the CNT-interconnect fabricated by the amount of 10 mL, 20 mL, and 80 mL CNT solution for the CNT network formation, respectively. In this study, we inferred the yield of the CNT-interconnects by randomly sampling ten CNT-interconnects for each condition. Basically, both figures demonstrate that the conductive probability of CNT-interconnects mostly decreases with the increase of the square number of the CNT-interconnect or the decrease of the times of coating cycles for the CNT network formation. However, the yield results show that under the same interconnect regime, part of the CNT-interconnects formed by the amount of 20 mL CNT solution has a higher yield than that formed by the amount of 80 mL CNT solution. This phenomenon could be attributed to the limited sticky ability of CNTs to the 1-nm-thick Al_2O_3 layer, so that the CNT density could not constantly accumulate within the interconnect regimes by such a spin coating method. In this experiment, we slowed down the spin speed to 100 rpm to keep the dropped CNT solution on the wafer as much as possible, and the well suspended CNTs in the solution were expected to uniformly deposit and form a CNT network after the evaporation of solvent during the baking process. With a total amount of 80 mL CNT solution, a highly dense CNT network could be fabricated, but the sticky ability from the CNTs in the relatively upper CNT network to the Al_2O_3 layer would be weak. Therefore, the CNTs are easily stripped during the following fabrication process, such as lithography process or lift off for patterning the bridge resistors. It is worthy to note that increasing the times of coating cycles would enhance the yield of CNT-interconnects with a relatively dimension. As shown in Fig. 4b, the maximum square number of CNT-interconnect fabricated by the amount of 10 mL CNT solution is 40 with the probability of 30%, while in the 20 mL case, the CNT-interconnects with 100 square numbers possess about 30% yield. In the last case, the amount of 80 mL CNT solution enhances the CNT-interconnects with 200 square numbers to have a 20% yield.

3.3. Characteristics of the CNT-interconnect conductance

Fig. 5 shows the fitting curves for average conductance of the width varying CNT-interconnects fabricated by the amount of 10 mL, 20 mL, and 80 mL CNT solution. Because of the quasi one-dimensional structure of the CNT, the conduction of the random distributed conductive sticks could be explained by percolation theory, in which the relation between the conductivity and the CNT density within a specified interconnect regime can be expressed as follows [31,32]:

$$\sigma \propto (N - N_c)^{\alpha}, \tag{1}$$

where σ represents the conductivity of the CNT-interconnect. N is the CNT density, and N_c is the critical CNT density corresponding to the percolation threshold. Above the critical density, it is possible for CNTs in a random configuration to connect conductive paths. The critical density for the CNT model is given by

$$l\sqrt{\pi N_c} = 4.236, \tag{2}$$

where l is the average length of the CNT. The formula (2) demonstrates that the critical density is a CNT length dependent parameter. As previously mentioned, the average CNT length is 3.5 μm, and then the critical density of a specified CNT interconnect regime can be approximately calculated as 0.466 CNTs/μm^2. The critical exponent, α, is a parameter depending only on geometry of the space.

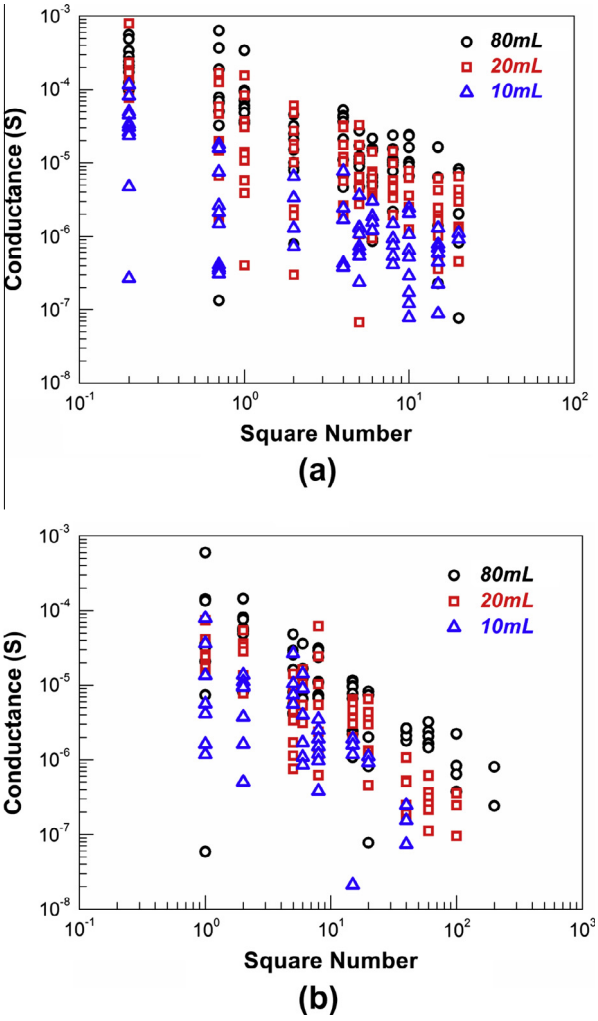

Fig. 3. Conductance distribution of the CNT-interconnects fabricated by the amount of 10 mL, 20 mL, and 80 mL CNT solution by slow spin rate coating and dry etching for (a) the CNT-interconnects in width varying set, (b) the CNT-interconnects in length varying set.

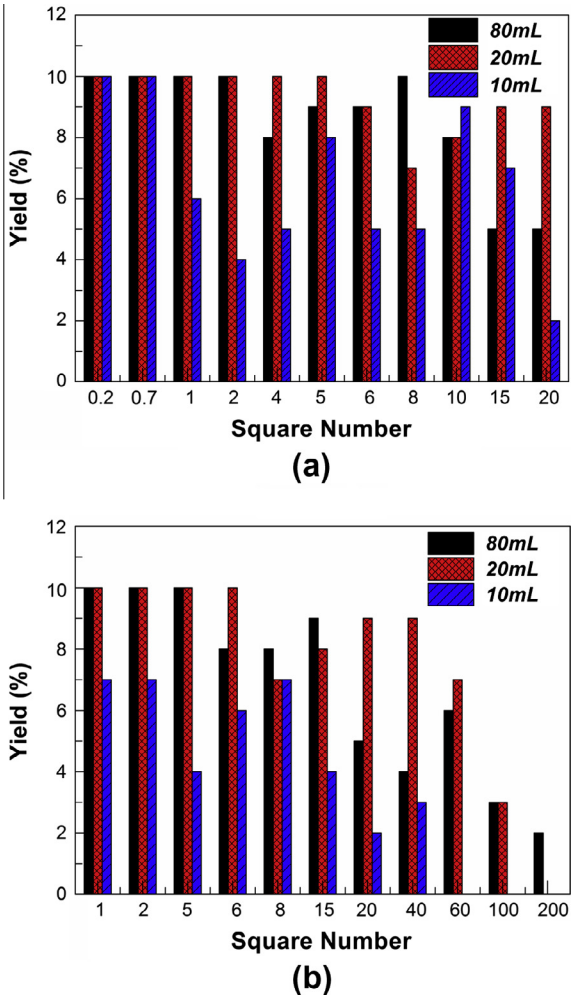

Fig. 4. Histograms of the number of working CNT-interconnects for (a) the CNT-interconnects in width varying set, (b) the CNT-interconnects in length varying set. 10 CNT-interconnects for each case were randomly sampled for statistics.

As determined in percolation theory, $\alpha = 1.33$ is for a two dimensional film [33]. The formula (1) was applied to fit the relation between the average conductance and the square number of the width varying CNT-interconnect as shown in Fig. 5. The proportionality constants corresponding to 10 mL, 20 mL, and 80 mL CNT solution for the CNT network formation are 1.53×10^{-5}, 1.33×10^{-4} and 4.25×10^{-4}, respectively. These proportionality constants are mainly involved with CNT self-resistance and tube-to-tube contact resistance, and this resistance originates from CNT diameter, species, chirality and defects, etc. [34]. Therefore, research has only discussed the critical density. In 2004, Hu et al. investigated the percolation phenomena in an ensemble of CNTs by using a filtration method to filter a dilute suspension of nanotubes in a solvent over a porous alumina filtration membrane (length 3 mm and width 5 mm) [35]. With the times of vacuum filtering increasing, more and more CNTs were stuck on the membrane and resulted in higher and higher probability of formation of CNT connected conductive paths. Eventually, they obtained the percolative relation between the conductance of the CNT networks on the porous alumina filtration membrane with cumulative CNT density. In our experiment, because of the thin layer of Al_2O_3 under the CNT networks, the CNTs would uniformly spread on the wafer by spin coating. Furthermore, CNT densities fabricated by slow spin rate coating were expected to be very dense, so CNTs per unit area could be reasonably assumed

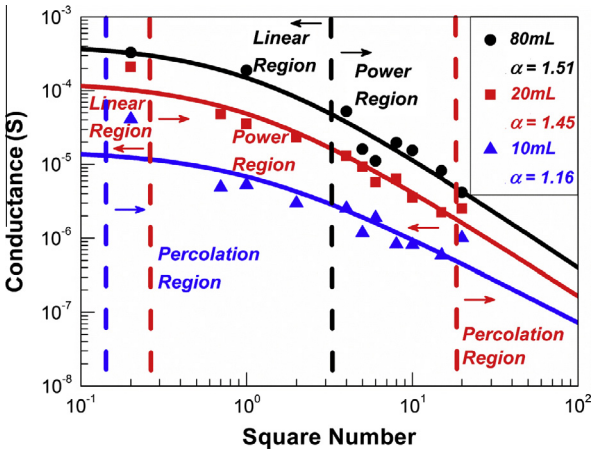

Fig. 5. The size dependent characteristics of the average conductance of the width varying CNT-interconnects fabricated by the amount of 10 mL, 20 mL, and 80 mL CNT solution by slow spin rate coating and dry etching. With the increase of times of coating cycle for CNT network formation, the phase transition phenomenon (percolation region–power region–linear region) is demonstrated.

as constant. However, such high density CNT networks were difficult to assess the density by manually counting, so we made a reasonable assumption that the average CNT density per unit area is

linearly proportional to the volume of solution applied to the spin coating to estimate the densities of the CNT networks. Therefore, the CNT density per unit area formed by 10, 20 and 80 mL CNT solution could be approximated as 4.25, 8.5 and 34 CNTs/μm^2. In terms of the probability, if the width of CNT-interconnect becomes wider, then electrodes have more chances to contact with CNTs. In addition, the electrodes are more likely to come across the CNTs aligned along the direction of two electrodes in the network and transport to the other electrode. Conversely, narrowing down the width would also lower the probability of the conduction of CNT-interconnects because some conducting paths in the network may be cut at the edge of interconnect. Therefore, with fixed lengths of CNT-interconnects, varying the CNT-interconnect width could have a similar effect as the change of the CNT density under specified times of coating cycles for CNT-interconnect formation. This implies the equivalence of the CNT density with the reciprocal of the square number of CNT-interconnect. In addition, we define the critical square number, S_c, which is analogous to the critical density, N_c, in the formula (1). That means, under specific times of coating cycles, the square number of CNT-interconnect less than critical square number would possess at least one conductive path.

Based on the above statement, the critical exponent of the power fitting curves for conductivity of the two dimensional CNT-interconnect, as a function of the reciprocal of square number about 1.33, means that the CNT connected paths in these CNT-interconnects forms a conductive plane. In this work, we classified the sizes of CNT-interconnects with such characteristics into power region. From Fig. 5, the exponent of the power fit is about 1.16 for the CNT-interconnect formed by the amount of 10 mL CNT solution. Referring to the approach proposed by Hu et al. in 2004, they found that the exponent, 1.5, of the power fit for the conductance of the CNT-interconnects with the increasing CNT densities came close to 1.33 after excluding some points around percolation region. We defined here the sizes of CNT-interconnects belonging to percolation region as the CNTs in the CNT-interconnect regime connect into only few conductive paths distributing sparsely in the CNT-interconnect regime. We also adopted a similar method to our results to investigate the power region. It is found that the exponents of fitting curves deviated from 1.33, as our fit includes less and less points excluding from the CNT-interconnects with $L \times W = 100\ \mu m \times 500\ \mu m$. This result interprets that all of the sampled CNT-interconnects in this case are classified into percolation region. As for the width varying CNT-interconnects fabricated by the amount of 20 mL CNT solution, the average conductance was fitted by a power function with the exponent 1.45. The best fit for the power region in this case is to exclude the points of the $100\ \mu m \times 500\ \mu m$ and $100\ \mu m \times 5\ \mu m$ interconnects. The result not only interprets that the square number of 20 is the critical square number of CNT-interconnects fabricated by the amount of 20 mL CNT solution, but it also shows that the $100\ \mu m \times 500\ \mu m$ CNT-interconnect should be sorted into another region, named linear region in this paper, in which the conductance of the CNT-interconnect would be linearly related with the square number of CNT-interconnects [36]. It is because the mutual contact resistance from tube-to-tube CNTs becomes influential, as the width of interconnect regime enlarges. Same power fit approach was applied to the CNT-interconnects formed by the amount of 80 mL CNT solution, and the exponent of the power function is fitted as 1.51. As the CNT-interconnects with the size of $100\ \mu m \times 500\ \mu m$ and $100\ \mu m \times 100\ \mu m$ were neglected, the exponent of the fitting curve became 1.27 which means that the CNT-interconnects with the size less than one square number belongs to linear region while other points are sorted into power region.

By the previously mentioned approach, the characteristics of the length varying CNT-interconnects fabricated by the amount of 10 mL, 20 mL, and 80 mL CNT solution are analyzed and shown in Fig. 6 with the proportionality constants 6.76×10^{-5}, 1.05×10^{-4} and 1.80×10^{-4}, respectively. In this case, the width of length varying CNT-interconnects is fixed at 5 μm, hence varying the length of CNT-interconnects could be viewed as the change of interconnect size. Again, the CNT per unit area could be viewed as constant owing to the uniformity of CNT distribution. Therefore, when the CNT-interconnect length was elongated, the CNTs would have less chance to connect to other CNTs and form conductive paths. Conversely, it is more likely to hold higher density of CNT conductive paths in shorter interconnects. Therefore, it is reasonable to conclude that the variation of CNT-interconnect length has a similar effect as the change of the CNT density under specified times of coating cycles for CNT-interconnect formation.

From Fig. 6, the exponent of the power related function for the interconnects with 10 mL of the CNT solution is about 1.49 which interprets that the CNT-interconnects with the sizes of $200\ \mu m \times 5\ \mu m$, $100\ \mu m \times 5\ \mu m$, and $75\ \mu m \times 5\ \mu m$ are sorted into percolation region. In addition, the critical square number of the CNT-interconnect fabricated by the amount of 10 mL of CNT solution could be approximated as 15. With the amount of 20 mL CNT solution, all sampled sizes of CNT-interconnects are classified into power region based on the 1.34 of exponent of the power dependent fitting curve. As for the case of 80 mL CNT solution, the result shows that all of the sampled results fall in the linear region. In addition, the average conductance of $5\ \mu m \times 5\ \mu m$ CNT-interconnects formed by the amount of 10 mL, 20 mL, and 80 mL CNT solution is approximately 2.02×10^{-5} S, 2.66×10^{-5} S and 1.15×10^{-4} S, respectively, which indicates better results than Zhenen Bao's group in 2011 by our simple fabrication process.

Furthermore, it is worthy to note that the increase of the average conductance of CNT-interconnects with the same size is not proportional to the times of coating cycles for CNT-interconnect formation. Such phase transition phenomena could also be explained by the percolation theory. The conductance of CNT-interconnect would surge quickly as power behavior with the increase of the CNT density and finally the density dependence would become linearly related as a conventional resistor. In this situation, the percolation theory could not be applicable to explain the conduction phenomena of the random distributed CNTs. Instead, the Ohm's law is comparatively appropriate to comprehend conductive behavior of CNT-interconnects with high density of CNTs.

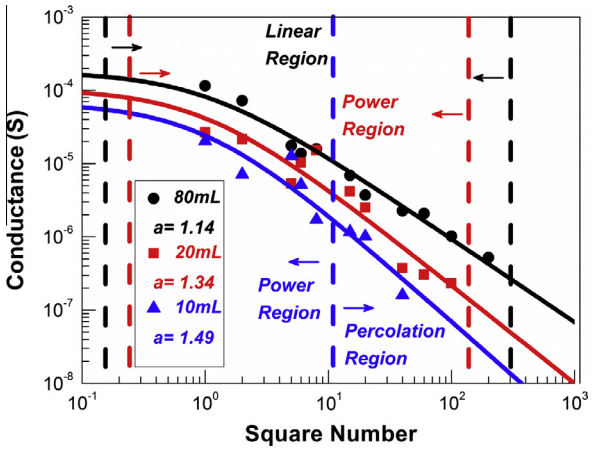

Fig. 6. The size dependent characteristics of the average conductance of the length varying CNT-interconnects fabricated by the amount of 10 mL, 20 mL, and 80 mL CNT solution by slow spin rate coating and dry etching. With the increase of times of coating cycle for CNT network formation, the phase transition phenomenon (percolation region–power region–linear region) is demonstrated.

This paper mainly focuses on the conductive mechanism and interconnect structure design of CNT-interconnects, and the reliability of CNT-interconnects is a critical issue and worth further researching. According to our preliminary experiments for CNT-interconnect reliability test, we discovered that the disconnection occurred at the contact between metal pad and CNTs, not at CNT tubes after long-time ejection of current through the CNT-interconnect. It is mainly because of that current crowding caused by the large difference between the width of a metal pad and the total width of CNTs. This non-homogeneous current density finally leads to electromigration at the metal/CNT contact.

4. Conclusions

In this work, we used slow spin rate coating and dry etching to fabricate the CNT-interconnects with various sizes. The size effect and the correlation between the size effect and the times of coating cycles were investigated. The results show that not only the amount of the CNT solution coated for forming the CNT network, but also the area of CNT-interconnect regime would affect the conductance, variation, and conductive probability of CNT-interconnects. Next, the yield of working CNT-interconnects does not show direct relation between the conductive probability with the times of coating cycles for CNT network formation. Finally, the power fitting approach applied to the average conductance and the reciprocal of the square number of CNT-interconnects under different conditions was shown and interpreted by percolation theory. In addition, we classified the characteristics of the average conductance of CNT-interconnects with different sizes into three categories: percolation region, power region and linear region. The phase transition phenomena were also demonstrated with the increase of the times of coating cycles. As the density of the CNT network increases continually, the conductance would enter the linear region and behaves as a conventional resistor.

Acknowledgements

The authors would like to thank the Nano Facility Center of National Chiao-Tung University for providing the experimental facilities. This work was supported in part by the Ministry of Education in Taiwan under ATU Program, and was supported in part by the National Science Council, Taiwan, ROC under the contract No.: NSC 100-2221-E-009-010-MY2.

References

[1] Lu L, Shen Y, Chen X, Qian L, Lu K. Ultrahigh strength and high electrical conductivity in copper. Science 2004;304:422–6.
[2] Liu HD, Zhao YP, Ramanath G, Murarka SP, Wang GC. Thickness dependent electrical resistivity of ultrathin (<40 nm) Cu films. Thin Solid Films 2001;384:151–6.
[3] Rossnagel SM, Kuan TS. Alteration of Cu conductivity in the size effect regime. J Vac Sci Technol 2004;B22:240–7.
[4] Chai Y, Chan PhCH, Fu Y, Chuang YC, Liu CY. Electromigration studies of Cu/carbon nanotube composite interconnects using blech structure. IEEE Electron Dev Lett 2008;29:1001–3.
[5] Andricacos PC. Copper on-chip interconnections, a breakthrough in electrodeposition to make better chips. Electrochem Soc Interface 1999:32–7.
[6] Andricacos PC, Uzoh C, Dukovic JO, Horkans J, Deligianni H. Damascene copper electroplating for chip interconnections. IBM J 1998;42:567–74.
[7] Ebbesen TW, Lezec HJ, Hiura H, Bennett JW, Ghaemi HF, Thio T. Electrical conductivity of individual carbon nanotubes. Nature 1996;382:54–6.
[8] Lee RS, Kim HJ, Fischer JE, Thess A, Smalley RE. Conductivity enhancement in single-walled carbon nanotube bundles doped with K and Br. Nature 1997;388:255–7.
[9] Frank S, Poncharal Ph, Wang ZL, de Heer WA. Carbon nanotube quantum resistors. Science 1998;280:1744–6.
[10] Tans SJ, Devoret MH, Dai H, Thess A, Smalley RE, Geerligs LJ, et al. Individual single-wall carbon nanotubes as quantum wires. Nature 1997;386:474–7.
[11] Yao Z, Kane ChL, Dekker C. High-field electrical transport in single-wall carbon nanotubes. Phys Rev Lett 2000;84:2941–4.
[12] Derycke V, Martel R, Appenzeller J, Avouris Ph. Carbon nanotube inter- and intramolecular logic gates. Nano Lett 2001;1:453–6.
[13] Tans SJ, Verschueren ARM, Dekker C. Room-temperature transistor based on a single carbon nanotube. Nature 1998;393:49–52.
[14] Javey A, Guo J, Farmer DB, Wang Q, Wang D, Gordon RG, et al. Carbon nanotube field-effect transistors with integrated ohmic contacts and high-k gate dielectrics. Nano Lett 2004;4:447–50.
[15] Radosavljevic M, Freitag M, Thadani KV, Johnson AT. Nonvolatile molecular memory elements based on ambipolar nanotube field effect transistors. Nano Lett 2002;2:761–4.
[16] Wind SJ, Appenzeller J, Martel R, Derycke V, Avouris Ph. Vertical scaling of carbon nanotube field-effect transistors using top gate electrodes. Appl Phys Lett 2002;80:3817–9.
[17] Tseng YC, Phoa K, Carlton D, Bokor J. Effect of diameter variation in a large set of carbon nanotube transistors. Nano Lett 2006;6:1364–8.
[18] Snow ES, Novak JP, Campbell PM, Park D. Random networks of carbon nanotubes as an electronic material. Appl Phys Lett 2003;82:2145–7.
[19] Kaempgen M, Duesberg GS, Roth S. Transparent carbon nanotube coatings. Appl Surface Sci 2005;252:425–9.
[20] Kymakis E, Amaratunga GAJ. Single-wall carbon nanotube/conjugated polymer photovoltaic devices. Appl Phys Lett 2002;80:112–4.
[21] Hur SH, Park OO, Rogers JA. Extreme bendability of single-walled carbon nanotube network transferred from high-temperature growth substrates to plastic and their use in thin-film transistors. Appl Phys Lett 2005;86:243502.
[22] Kang SJ, Kocabas C, Ozel T, Shim M, Pimparkar N, Alam MA, et al. High-performance electronics using dense, perfectly aligned arrays of single-walled carbon nanotubes. Nature 2007;2:230–6.
[23] Freitag M, Johnson AT, Kalinin SV, Bonnell DA. Role of single defects in electronic transport through carbon nanotube field-effect transistors. Phys Rev Lett 2002;89:216801.
[24] Lyons PE, Sukanta De, Blighe F, Nicolosi V, Felipe L, Pereira C, et al. The relationship between network morphology and conductivity in nanotube films. J Appl Phys 2008;104:044302.
[25] Hellstrom SL, Vosgueritchian M, Stoltenberg RM, Irfan I, Hammock M, Wang YB, et al. Strong and stable doping of carbon nanotubes and graphene by MoO_x for transparent electrodes. Nano Lett 2012;12:3574–80.
[26] Lin DW, Bettinger CJ, Ferreira JP, Wang CL, Bao Z. A cell-compatible conductive film from a carbon nanotube network adsorbed on poly-L-lysine. ACS Nano 2011;5:10026–32.
[27] Chang HY, Tsui BY. Low-temperature wafer-scale fabrication of carbon nanotube network thin-film transistors: geometry effect and transport mechanism. In: The 4th IEEE international nanoelectronics conference (INEC), vol. B3-4; June 2011. p. 21–4.
[28] Lee TC, Tsui BY, Tzeng PJ, Wang CC, Tsai MJ. An optimized process for high yield and high performance carbon nanotube field effect transistors. Microelectron Reliab 2010;50(5):666–9.
[29] Dresselhaus MS, Jorio A, Souza Filho AG, Dresselhaus G, Saito R. Raman spectroscopy on one isolated carbon nanotube. Physica B 2002;323:15–20.
[30] Fuhrer MS, Nygard J, Shih L, Forero M, Yoon Young-Gui, Mazzoni MSC, et al. Crossed nanotube junctions. Science 2000;288:494–7.
[31] Pike GE, Seager CH. Percolation and conductivity L A computer study I. Phys Rev 1974;10(B):1421–34.
[32] Seager CH, Pike GE. Percolation and conductivity L A computer study II. Phys Rev 1974;10(B):1435–46.
[33] Stauffer D, Aharony A. Introduction to percolation theory. London: Taylor & Francis; 1993.
[34] Stadermann M, Papadakis SJ, Falvo MR, Novak J, Snow E, Fu Q, et al. Nanoscale study of conduction through carbon nanotube networks. Phys Rev B 2004;69:201402.
[35] Hu L, Hecht DS, Gruner G. Percolation in transparent and conducting carbon nanotube networks. Nano Lett 2004;4:2513–7.
[36] Wang Q, Dai J, Li W, Wei Z, Jiang J. The effects of CNT alignment on electrical conductivity and mechanical properties of SWNT/epoxy nanocomposites. Compos Sci Technol 2008;68:1644–8.